

## Acoustic phonon scattering in $\text{Bi}_2\text{Te}_3/\text{Sb}_2\text{Te}_3$ superlattices

Yaguo Wang,<sup>1</sup> Carl Liebig,<sup>1</sup> Xianfan Xu,<sup>1(a)</sup> and Rama Venkatasubramanian<sup>2</sup>

<sup>1</sup>*School of Mechanical Engineering and Birck Nanotechnology Center, Purdue University, West Lafayette, Indiana 47907, USA*

<sup>2</sup>*Center for Solid State Energetics, RTI International, Research Triangle Park, North Carolina 27709, USA*

(Received 6 June 2010; accepted 8 August 2010; published online 24 August 2010)

Ultrafast time-resolved measurements were conducted to investigate long-wavelength acoustic phonon scattering and velocity reduction in  $\text{Bi}_2\text{Te}_3/\text{Sb}_2\text{Te}_3$  superlattices. We show that both these phenomena suppress heat transfer process, with the phonon scattering contributing more in differentiating the lattice thermal conductivities among films with different periods. Measurements of reduction in the acoustic phonon amplitudes support the decrease in the thermal conductivity for certain superlattice periods, which is not predicted by acoustic mismatch theory. This study is a direct measurement of coherent acoustic phonons in superlattices which is of significant interest to thermoelectrics. © 2010 American Institute of Physics. [doi:10.1063/1.3483767]

Thermoelectric materials are often characterized using the figure of merit,  $ZT = S^2 \sigma T / \kappa$ , where  $T$  is the temperature,  $S$  the Seebeck coefficient,  $\sigma$  the electrical conductivity, and  $\kappa$  the thermal conductivity. To improve the figure of merit, a significant amount of studies have been focused on reducing the lattice thermal conductivity through increasing phonon scattering by engineering superlattices,<sup>1</sup> filled cage-like structures (i.e., skutterudites<sup>2,3</sup>), nanowires,<sup>4</sup> and nanograins.<sup>5</sup> Thin-film superlattices (SLs) are promising candidates with a reported  $ZT = 2.4$  in the p-type  $\text{Bi}_2\text{Te}_3/\text{Sb}_2\text{Te}_3$  superlattice.<sup>1</sup> Several theoretical models have been used to explain the reduction in the lattice thermal conductivity in SLs. Possible mechanisms are scattering at interfaces,<sup>6</sup> which shortens the phonon mean free path, quantum confinement effects, which reduce the phonon group velocity perpendicular to the SL layers by flattening the acoustic phonon dispersion curves,<sup>7</sup> and a weak localization of phonons inferred from a characteristic minimum in thermal conductivity at certain periods in  $\text{Bi}_2\text{Te}_3/\text{Sb}_2\text{Te}_3$  SLs (Ref. 8) which has also been observed in other material systems. Theoretical work on GaAs/AlAs SLs suggests that lower phonon velocities contribute to approximately 30% of the total thermal conductivity reduction, while the remainder is attributed to the shorter phonon mean free path.<sup>7</sup> Direct measurements of optical phonons in  $\text{Bi}_2\text{Te}_3$  thin films and interface scattering of optical phonons in p-type  $\text{Bi}_2\text{Te}_3/\text{Sb}_2\text{Te}_3$  SLs have been reported recently.<sup>9,10</sup> On the other hand, to investigate heat transport, studies of acoustic phonons are also necessary.

In this work, we use ultrafast time-resolved pump-probe methods to investigate long-wavelength coherent acoustic phonons in  $\text{Bi}_2\text{Te}_3/\text{Sb}_2\text{Te}_3$  SLs. For an opaque material, ultrafast optical pulses locally heat a near-surface layer, which expands, creating a coherent acoustic phonon wave propagating away from the surface.<sup>11</sup> The propagation and scattering of the coherent acoustic phonons can be detected using ultrafast pump-probe techniques by monitoring changes in the surface reflectivity when the coherent acoustic phonon wave is reflected from the back surface of the sample or from the film-substrate interface. The differences of acoustic pho-

non propagation in SL samples versus those in their bulk counterparts are investigated and compared to determine the role of interface scattering in the SL films.

The experiments were performed using a standard two-color pump-probe scheme. Details of experiments have been documented in previous publications.<sup>3,9,10</sup> Samples investigated in this study are listed in Table I. All the films are much thicker than their absorption depth at 800 and 400 nm laser wavelengths (tens of nm). The films were grown using metal-organic chemical-vapor deposition (MOCVD) on GaAs (100) substrates along the c-axis of the films.<sup>12</sup> The SL samples have alternating  $\text{Bi}_2\text{Te}_3$  layer and  $\text{Sb}_2\text{Te}_3$  layer in each period. A  $\text{Bi}_2\text{Te}_3$  buffer layer was deposited between the SL and the substrate. An additional 7 nm thick  $\text{Sb}_2\text{Te}_3$  film is deposited onto the top of all the samples.

An example of changes in reflectivity caused by acoustic phonons measured in sample SL3/3I is shown in Fig. 1. The initial echo is the partial reflection from the SL-buffer interface and the second is the partial reflection from the buffer-substrate interface. The acoustic waves spread over a time duration of approximately 50 ps, which corresponds to a wavelength of about 125 nm (estimated using the phonon velocity of 2500 m/s). At room temperature, most phonons are populated at the edge of the first Brillouin zone, where the phonons have shorter wavelengths and the phonon group velocities can be smaller than the sound velocity.<sup>6</sup> It was shown in a recent numerical study on wavelength-dependent thermal conductivity in bulk silicon<sup>13</sup> that long-wavelength phonons also contribute to thermal conductivity. Therefore,

TABLE I. List of samples studied in this paper.

Nominal name	Components	$\text{Bi}_2\text{Te}_3$ buffer ( $\mu\text{m}$ )	Thickness ( $\mu\text{m}$ )/periods
$\text{Bi}_2\text{Te}_3\text{I}$	$\text{Bi}_2\text{Te}_3$ film		0.59
$\text{Bi}_2\text{Te}_3\text{II}$	$\text{Bi}_2\text{Te}_3$ film		1.12
SL1/II	$\text{Bi}_2\text{Te}_3(1 \text{ nm})/\text{Sb}_2\text{Te}_3(1 \text{ nm})$	0.134	0.56/213
SL1/III	$\text{Bi}_2\text{Te}_3(1 \text{ nm})/\text{Sb}_2\text{Te}_3(1 \text{ nm})$	0.120	1.44/660
SL3/3I	$\text{Bi}_2\text{Te}_3(3 \text{ nm})/\text{Sb}_2\text{Te}_3(3 \text{ nm})$	0.130	0.49/60
SL3/3II	$\text{Bi}_2\text{Te}_3(3 \text{ nm})/\text{Sb}_2\text{Te}_3(3 \text{ nm})$	0.140	1.43/215
SL2/2	$\text{Bi}_2\text{Te}_3(2 \text{ nm})/\text{Sb}_2\text{Te}_3(2 \text{ nm})$	0.145	1.05/226
SL1/5	$\text{Bi}_2\text{Te}_3(1 \text{ nm})/\text{Sb}_2\text{Te}_3(5 \text{ nm})$	0.142	1.49/225

<sup>a</sup>Electronic mail: xxu@ecn.purdue.edu. Tel.: 1-765-494-5639. FAX: 1-765-494-0539.

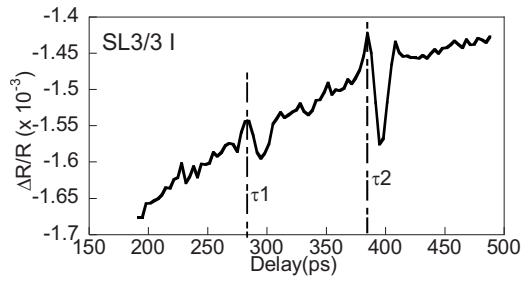


FIG. 1. Typical coherent acoustic phonon signals detected in SL samples.

studies of long-wavelength phonon scattering can provide insight to the understanding of the thermal conductivity in SL films.

Figure 2 shows coherent acoustic phonon signals measured in three sets of samples: two bulk  $\text{Bi}_2\text{Te}_3$  films, two SL1/1 SL films, and two SL3/3 films after removing the non-oscillatory thermal background. It can be seen that as the film thickness increases, there is no measurable change in the phonon amplitude in the bulk  $\text{Bi}_2\text{Te}_3$  thin films. On the other hand, the phonon amplitude decreases of about 40% and 50% for the SL1/1 and SL3/3 samples when the film thickness is increased. Therefore, there is much stronger scattering in  $\text{Bi}_2\text{Te}_3/\text{Sb}_2\text{Te}_3$  SLs compared to the bulk  $\text{Bi}_2\text{Te}_3$  films. Similar enhanced scattering of optical phonons in  $\text{Bi}_2\text{Te}_3/\text{Sb}_2\text{Te}_3$  SLs has been reported previously.<sup>9</sup> The stronger scattering in SL3/3 compared to SL1/1 is noteworthy and

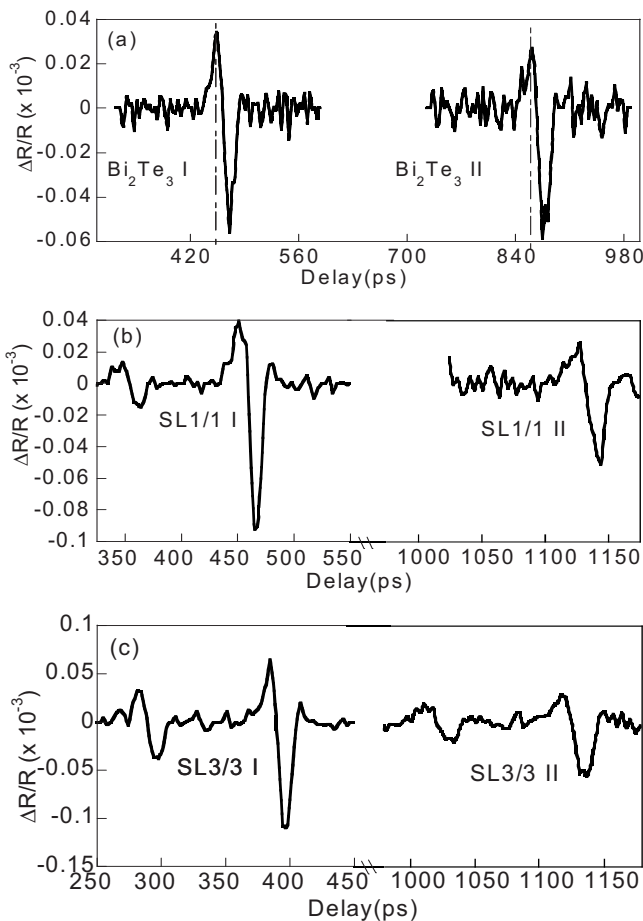


FIG. 2. Coherent acoustic phonon signals after removal of background in (a)  $\text{Bi}_2\text{Te}_3$  thin films, (b)  $\text{Bi}_2\text{Te}_3$ (1 nm)/ $\text{Sb}_2\text{Te}_3$ (1 nm) SL films, and (c)  $\text{Bi}_2\text{Te}_3$ (3 nm)/ $\text{Sb}_2\text{Te}_3$ (3 nm) SL films.

is consistent with thermal conductivity measurements reported in this SL system.<sup>8</sup>

The acoustic velocities in the SL films can be calculated from the film thicknesses and the arrival times of acoustic phonon peaks, marked by the dashed lines in Fig. 2(a) for samples  $\text{Bi}_2\text{Te}_3\text{I}$  and  $\text{Bi}_2\text{Te}_3\text{II}$ . The velocities of acoustic phonons in these two bulk films are calculated to be 2600 m/s, which are consistent with the bulk value. Velocities in SL films will be discussed in detail later.

Reflection of acoustic phonons at an interface can be estimated using the acoustic mismatch theory, as follows:<sup>14</sup>

$$r = \frac{Z_\alpha - Z_\beta}{Z_\alpha + Z_\beta} = \frac{(\rho_\alpha v_\alpha - \rho_\beta v_\beta)}{(\rho_\alpha v_\alpha + \rho_\beta v_\beta)}, \quad (1)$$

where  $Z$  is the acoustic impedance calculated as  $\rho v$ ,  $\rho$  is the density, and  $v$  is the longitudinal acoustic phonon velocity.  $\alpha$  and  $\beta$  represent the materials before and after the interface (in our case  $\text{Bi}_2\text{Te}_3$ ,  $\text{Sb}_2\text{Te}_3$ , and GaAs substrate). The densities of bulk  $\text{Bi}_2\text{Te}_3$ ,  $\text{Sb}_2\text{Te}_3$ , and GaAs substrate are 7.86 g/cm<sup>3</sup>, 6.505 g/cm<sup>3</sup>, and 5.32 g/cm<sup>3</sup>, respectively; and the acoustic velocities are 2600 m/s, 2900 m/s,<sup>15</sup> and 4731 m/s,<sup>16</sup> respectively. Using Eq. (1), the decrease in phonon amplitude (after passing through all interfaces) is 95% in SL1/1 films and 60% in SL3/3 films. These results do not agree with those obtained from the experiments, especially for the SL1/1 films—much stronger acoustic phonon scattering was obtained from Eq. (1). The reason for this discrepancy is due to the assumption in the acoustic mismatch theory that the two materials constituting the interface are semi-infinite. In SLs, the transmittance (reflectance) at interfaces is not only determined by the properties of two contacting materials, but also the difference between the characteristic thickness of the SL layers and the phonon wavelength. It has been shown numerically that when the phonon wavelength is long compared with the characteristic thickness of the SL layers, the transmission increases.<sup>17</sup> In our experiments, the wavelength of acoustic phonons generated with ultrafast pulses ( $\sim 125$  nm) is much longer than the periodicity of the SLs (2 and 6 nm). Therefore, scattering of phonons with such long wavelengths is considerably weakened, in contrast to the prediction from the simple acoustic mismatch theory. Additionally, imperfections in SLs also contribute to scattering. With this consideration, there is an even larger discrepancy between the calculated and measured scattering at SL interfaces.

In SL, along the growth direction, phonon branches in the first Brillouin zone are folded. This folding produces two consequences: first, minibands and hence anticrossings are formed at the center and edge of the SL Brillouin zone. Second, the phonon dispersion curves are flattened, which lowers the phonon group velocity.<sup>7</sup> With the measured arrival times of acoustic echoes and SL film thicknesses, the corresponding longitudinal phonon group velocities were calculated and plotted in Fig. 3 as a function of single-period thickness of SL. The solid symbols in Fig. 3 show the measured acoustic velocities of samples with different SL periods: 1/1, 2/2, 1/5, and 3/3. The phonon group velocities in the two SL films with the same single-period thickness of 6 nm are almost the same, while the acoustic velocity tends to decrease slightly with the decrease in the SL period, which has been reported in the Cu/W multilayer structures.<sup>18</sup> The

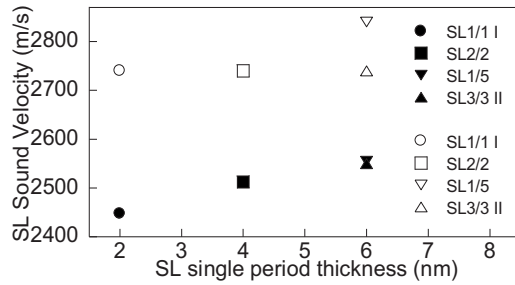


FIG. 3. Effective acoustic velocities in  $\text{Bi}_2\text{Te}_3$  SLs as a function of thickness of one SL period. The solid symbols are experimental results and the open symbols are values calculated using Eq. (2).

effective sound velocity,  $v_{\text{eff}}$ , in a multilayer structure can be evaluated using the following expression:<sup>18</sup>

$$v_{\text{eff}} = \frac{d}{\sqrt{\frac{d_1^2}{v_1^2} + \frac{d_2^2}{v_2^2} + \left(\frac{Z_1}{Z_2} + \frac{Z_2}{Z_1}\right) \frac{d_1 d_2}{v_1 v_2}}}, \quad (2)$$

where  $d_1$ ,  $d_2$ ,  $v_1$ ,  $v_2$ , and  $Z_1$ ,  $Z_2$  stand for the thickness, sound velocity, and acoustic impedance, respectively.  $d = d_1 + d_2$  is the single period thickness. The effective velocities calculated using Eq. (2) are plotted as open symbols in Fig. 3. It is seen that the measured acoustic velocities are lower than the values calculated using Eq. (2) for all the SL films by about 10%, and this reduction partially contributes to lowering the lattice thermal conductivity in the SL films, which was predicted as a result of flattened phonon dispersion curve.<sup>7</sup>

It is noted that although the acoustic velocities in SLs are smaller than the theoretical values estimated from Eq. (2), the differences are quite small. On the other hand, there is a relatively large difference in the phonon amplitudes: the amplitudes of coherent phonons in SL2/2 and SL1/5 films are about 70% and 60% of that in the SL1/1 films. Experimentally, it was found that the lattice thermal conductivity in the  $\text{Bi}_2\text{Te}_3/\text{Sb}_2\text{Te}_3$  SL are 0.48 W/mK in SL1/1, 0.23 W/mK in the SL2/2, and 0.25 W/mK in the SL1/5 films.<sup>8</sup> Therefore, it appears that acoustic phonon scattering plays a dominant role in thermal conductivities of SL films with different periods.

In summary, we conducted ultrafast time-resolved coherent acoustic phonon measurements in  $\text{Bi}_2\text{Te}_3/\text{Sb}_2\text{Te}_3$  SL films. Scattering of long-wavelength acoustic phonons was

investigated, and scattering from interfaces in SLs was observed. The acoustic phonon amplitude measurements support the observation of minimum thermal conductivity at certain SL periods,<sup>8</sup> and deviations from acoustic mismatch theory<sup>14</sup> were noted. This study represents a direct measurement of coherent acoustic phonon scattering in SLs which is of significant interest to nanoscale thermal transport and thermoelectrics.

We would like to acknowledge the support to this work by the Defense Advanced Research Project Agency (DARPA), the Sandia National Laboratory, and the Air Force Office of Scientific Research (AFOSR). The thin-film samples were grown by Mr. Thomas Colpitts at RTI International under a DARPA/DSO Army Contract No. W911NF-08-C-0058, which is gratefully acknowledged.

<sup>1</sup>R. Venkatasubramanian, E. Siivola, T. Colpitts, and B. O'Quinn, *Nature (London)* **413**, 597 (2001).

<sup>2</sup>B. C. Sales, D. Mandrus, and R. K. Williams, *Science* **272**, 1325 (1996).

<sup>3</sup>Y. Wang, X. Xu, and J. Yang, *Phys. Rev. Lett.* **102**, 175508 (2009).

<sup>4</sup>A. I. Hochbaum, R. Chen, R. D. Delgado, W. Liang, E. C. Garnett, M. Najarian, A. Majumdar, and P. Yang, *Nature (London)* **451**, 163 (2008).

<sup>5</sup>B. Poudel, Q. Hao, Y. Ma, Y. Lan, A. Minnich, B. Yu, X. Yan, D. Wang, A. Muto, D. Vashaee, X. Chen, J. Liu, M. S. Dresselhaus, G. Chen, and Z. Ren, *Science* **320**, 634 (2008).

<sup>6</sup>G. Chen, *Phys. Rev. B* **57**, 14958 (1998).

<sup>7</sup>W. E. Bies, R. J. Radtke, and H. Ehrenreich, *J. Appl. Phys.* **88**, 1498 (2000).

<sup>8</sup>R. Venkatasubramanian, *Phys. Rev. B* **61**, 3091 (2000).

<sup>9</sup>Y. Wang, X. Xu, and R. Venkatasubramanian, *Appl. Phys. Lett.* **93**, 113114 (2008).

<sup>10</sup>A. Q. Wu, X. Xu, and R. Venkatasubramanian, *Appl. Phys. Lett.* **92**, 011108 (2008).

<sup>11</sup>T. Saito, O. Matsuda, and O. B. Wright, *Phys. Rev. B* **67**, 205421 (2003).

<sup>12</sup>R. Venkatasubramanian, T. Colpitts, E. Watko, M. Lamvik, and N. El-Masry, *J. Cryst. Growth* **170**, 817 (1997).

<sup>13</sup>A. S. Henry and G. Chen, *J. Comput. Theor. Nanosci.* **5**, 141 (2008).

<sup>14</sup>L. E. Kinsler, A. R. Frey, A. B. Coppens, and J. V. Sanders, *Fundamentals of Acoustics* (Wiley, New York, 1981).

<sup>15</sup>J. S. Dyck, W. Chen, and C. Uher, *Phys. Rev. B* **66**, 125206 (2002).

<sup>16</sup>J. S. Blakemore, in *Numerical Data and Functional Relationships in Science and Technology*, Landolt-Börnstein, Group III Condensed Matter, Vol. 41 edited by O. Madelung, M. Schulz, and H. Weiss (Springer, Berlin, 1983).

<sup>17</sup>Z. Huang, J. Murthy, and T. Fisher, Proceedings of ASME 2008 Heat Transfer Summer Conference, Florida, 2008, p. 557.

<sup>18</sup>B. Bonello, B. Perrin, E. Romatet, and J. C. Jeannet, *Ultrasonics* **35**, 223 (1997).